Estimating the spatial distribution of vegetation height and ground-level elevation in a mesotidal salt marsh from UAV LiDAR-derived point cloud

Daniele Pinton[§], Alberto Canestrelli, Christine Angelini, Benjamin Wilkinson, Peter Ifju, Andrew Ortega

University of Florida
Department of Civil and Coastal Engineering
1949 Stadium Road, Gainesville, FL, USA
[§] daniele.pinton@ufl.edu

Abstract— **Salt marshes are transitional wetlands placed between ocean and land, which act as natural defenses against coastal hazards. The amount of organic and inorganic deposition, which is strongly influenced by vegetation characteristics, is one of the main drivers for the survival of salt marshes. Vegetation also favors the dissipation of wind waves and storm surges. For these reasons, an accurate description of canopy characteristics in salt marshes is critical for their preservation and management. For this purpose, airborne LiDAR (Light Detection And Ranging) has become an accessible and cost-efficient tool to map large wetland areas. However, the limited horizontal resolution of airborne-derived point clouds (~1 m) prevents the direct extraction of ground elevation and vegetation height if not coupled with other data sources, such as RGB or hyperspectral images. Uncrewed Aerial Vehicles (UAV) have become an affordable and cost-efficient tool to map targeted salt marshes quickly. Although LiDAR is capable of measuring surface elevations, laser penetration is limited in dense salt marsh vegetation. The limited ability of the laser to penetrate dense vegetation hinders its usefulness for surveying tidal marsh platforms. For UAV-borne LiDAR, a reliable method to extract ground elevation and vegetation height from high-resolution point clouds is yet not available. Here we derive a new formulation for converting the 3D distribution of UAV derived points into vegetation height and ground-level elevation without the support of other data sources. Our formulation has been calibrated on the surveyed vegetation height in a *Spartina alterniflora* marsh in Little Sapelo Island, Georgia, USA, and successfully tested on an independent dataset. Our method produces high-resolution (40×40 cm²) maps of ground elevation and vegetation height, thus capturing the large gradients in the proximity of tidal creeks.**

I. INTRODUCTION

The increased interest in wetland health is related to their progressive degradation and conversion in open water areas and mudflats. The leading causes of these transformations are the human interaction and the increasing sea-level rise [1]. As estuarine wetlands, salt marshes are an essential environment for many ecological, anthropologic, and economic reasons. They protect shorelines from storms, sequester carbon, improve water quality, and provide habitat for fisheries [2]–[4]. Salt marshes are the result of ecological and physical interactions [5], which requires numerical modeling to quantify the connections between hydrodynamic, morphological, and environmental processes [6], usually interested by non-linear effects. Long term evolution of salt marshes is characterized using empirical models. However, short term evolution processes that require higher precision are described using physical models [7]. In both cases, vegetation plays a central role, mitigating the effect of the meteorological agents and modulating the sedimentation and flooding patterns in the marsh area [8], [9]. In particular, vegetation influences the vertical flow velocity, producing additional frictional forces. These forces are mainly based on vegetation characteristics, such as the thickness of the vegetation layer that is strongly correlated to the ground-level elevation. Considering these reasons, an accurate description of both ground elevation and vegetation in salt marshes is essential for their management and conservation. LiDAR technology has been successfully used for many applications in wetlands, such as mapping forested wetlands [10] and quantifies the effects of sea-level rise in coastal salt meadows [11]. However, Airborne LiDAR data may not provide adequate representation of the creek network on the marshes [12], due to the low resolution of the surveyed datasets (~1 m). Unmanned Aerial Vehicle (UAV) is becoming a standard technology used for numerous purposes, such as high-resolution mapping [13], agricultural [14], and shoreline surveys [15], as well as for the estimation of vegetation biomass [16], [17]. More precise representation of the complex salt marsh morphodynamic and biological properties, as the vegetative cover [18] can be obtained using UAV-borne LiDAR point clouds, which higher resolution (~5 cm), is due to the lower flight altitude and the higher laser pulsation frequency.

The objective of this study is the production of high resolution (40×40 cm²) maps of ground elevation and vegetation height using UAV-borne LiDAR, to describe the complexity of the tidal network crossing the salt marshes. With this goal, we derived a new formulation that converts UAV-based LiDAR point clouds into ground-level elevation and vegetation height. Our formulation has been calibrated

from surveyed height data on a 0.26 km^2 *Spartina alterniflora* salt marsh in Little Sapelo Island, Georgia, USA. *S. alterniflora* is the predominant macrophyte in this area [1]. Its stems range from 20 cm to 2 m in height. While short *S. alterniflora* occupies the higher marsh platform with stem heights of 0.20–0.60 m, tall Spartina fills the lower marsh and creek banks with heights up to 2 m. The results were successfully tested on an independent dataset. The determination of more accurate and high-precision vegetation and topographic characteristics will be beneficial for the numerical description of coastal wetlands processes.

II. METHODS

A. Measurements

Field measurements were carried out on the 22nd of November 2019, in conjunction with a UAV-LiDAR survey. The data were acquired during a low tide event to avoid the effects of the tide on the survey.

Twenty-seven Ground Control Points (GCPs) were positioned on the marsh. Their geographic coordinates were measured to verify the accuracy of the acquired LiDAR point cloud. The vertical elevation and geographic position data were collected during a high-precision RTK-GPS survey. Their position was decided to cover the marsh domain homogeneously, allowing a proper verification of the accuracy of the collected LiDAR point cloud. The GCPs were placed 1 m above the ground level to make them visible for the surveying staff and to avoid to be covered by the tall vegetation and high tide.

Sixty-eight 40×40 cm^2 plots were randomly set in the study area, and their geographic coordinates and vertical elevation were surveyed. The spatial distribution of the plots was decided to cover all the marsh domain and to collect homogeneously distributed values in the plausible range of the measured vegetation height (~0.20-2.00 m). Each plot was located in a homogeneous area in terms of elevation and vegetation height. The vegetation height was measured, collecting the length of three *Spartina alterniflora* stems. The minimum, the mean and the maximum values of vegetation height were recorded. To confirm the measured data, we collected RGB images using a field-based tool for measurement, made of: (i) a wooden panel at a 45-degree angle to the ground, (ii) a horizontal-looking Distianert 12 megapixel Trail Camera with 80 m detection range, and a 125° field of view, connected to the panel and (iii) a red background board with a calibration scale [19]. The elevation and position data were collected using an RTK-GPS (Trimble R6 GNSS ±2 cm vertical and ±1 cm maximum horizontal accuracy) in the Universal Traversal Mercator (UTM) WGS84 17N reference system. The elevation data were measured with respect to the WGS84 ellipsoid.

We surveyed the study area with a UAV-borne LiDAR on the 22nd of November 2019, during a low tide event, to minimize the effects of the tide on LiDAR survey. The LiDAR system used to acquire the data employed a Velodyne VLP-16 Puck Lite. This scanner is comprised of 16 beams and acquires 600,000 points per second by including dual returns. The scanner is georeferenced with a Novatel STIM-300 Intertial Measurement Unit and GNSS receiver. The GNSS data were post-processed using a local base station. This local base station data was processed using OPUS (https://www.ngs.noaa.gov/OPUS/) to provide an accurate solution to enable PPK processing. (Post Processed Kinematics). This system is mounted on a DJI M600 airframe, which has an average of 20 minute flight time and is capable of flying pre-programmed waypoint missions. This flight was operated at 40 m altitude with 50 m flight line spacing. The acquired point cloud has an average density of ~500 points/m^2.

To maximize the accuracy in vegetation and ground-level elevation description, the acquired point cloud was filtered by applying two cut-off filters, removing: (i) the points with an elevation higher than 2.50 m above the MSL and lower than 1.20 m below the MSL, that describe the freshwater forest placed at the north-western boundary of the domain and the surface of the Duplin River, respectively and (ii) the points collected outside the study area. Both filters were performed using the CloudCompare software.
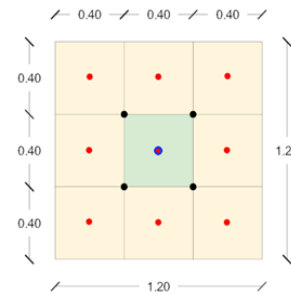
Figure 1. 3×3 cell stencil used in the determination of ground level elevation. The ground-level elevation in the central cell indicated as *(n,e)* was calculated using the eight surrounding yellow cells. The red dots are the minimum elevation values detected in every 0.4×0.4 m^2 cell. The black dots are the values calculated in the fourth step. The blue central dot is the final ground elevation level defined in the stencil.

B. Parameters estimation

Once filtered, LiDAR data were associated with the RTK-GPS data and the vegetation heights surveyed in the marsh, to define possible relations. Sixty-eight smaller point clouds were extracted and analyzed in the neighborhood of each surveyed plot. To calculate the ground-level elevation, the domain area and the LiDAR dataset were divided into 0.40 m × 0.40 m cells, using a 2737×1379 grid, whose gridlines were oriented in the North and East directions. Each cell location was identified by two indexes, (*n*) and (*e*) (north and east). The ground level in the salt marsh domain was calculated considering the local distribution of the minimum elevation values collected by the UAV-based LiDAR in a 3x3 cell stencil centered in *(n,e),* corresponding to a square 1.20x1.20m^2 area (Figure 1). The procedure was implemented based on the following assumption: since over the marsh the gradients in ground elevation are small, cells larger than 0.4x0.4 m^2 have a higher probability that at least one laser beam bypasses the vegetation and reaches the ground, thus reducing the error in estimating the real ground elevation by using the minimum elevation of the point cloud within the cell. The effects of the creeks, the holes, and sometimes the adverse impact stagnant water can have on the reflected laser beam, inevitably decrease the amount of the minimum elevation detected in their proximity using the overlying point cloud. To avoid that, we analyzed the distribution of the elevation values collected with the point cloud, using the following workflow for every *(n,e)* cell.

The algorithm developed to describe the ground-level elevation starting from the collected point cloud is based on the following steps:

1. **STEP 1**: Once the LiDAR dataset was split into *(n,e)* subsets, indicated as $PC_{n,e}$.
2. **STEP 2**: the elevation and the geographic coordinates of the lowest point in each *(n,e)* cell were identified and placed in the cell's centroids (red dots, Figure 1). The minimum elevation value was calculated as:

$$z_{\min,n,e} = min[h_k] \qquad h_k \in PC_{n,e} \qquad (1)$$

where h_k is the elevation of the k points contained in the $PC_{n,e}$ subset.

3. **STEP 3**: For each *(n,e)* cell, a regression plane was determined using the geographic position of the lowest points detected in its 3×3 cells stencil (red dots in Figure 1). The mean slope of the plane ($S_{n,e}$) and the vertical range of the nine minimum elevation points ($R_{n,e}$) for each stencil were calculated as:

$$S_{n,e} = (|S_n| + |S_e|)/2 \qquad (2)$$

$$R_{n,e} = max[z_{\min,i,j}] - min[z_{\min,i,j}] \qquad (3)$$
$$i = 1,3; \quad j = 1,3$$

where S_n and S_e are the slope in the two main directions (east and north) of the regression plane of each *(n,e)* cell.

4. **STEP 4**: Two elevation values were attributed to the four vertexes of the central cell (black dots in Figure 1) of the 3×3 stencil. These values correspond to the minimum and the mean z_{min} calculated in the four cells surrounding each vertex. Two additional regression planes were determined from the two calculated datasets. The midpoint elevation of the two planes indicated as $Mean_{zmin,}$ and Min_{zmin} respectively, were calculated and placed in the middle of the 3×3 stencil.
5. **STEP 5**: The cells close to the creeks were identified using a threshold of 0.30 on the slope and 0.30 m on the vertical range, calculated as described at STEP 3. The thresholds were chosen, analyzing the shape of the point cloud in the proximity of the creeks. The ground elevation value ($Z_{G,n,e}$) of the *(n,e)* cells was calculated as follows:

$$\begin{cases} Z_{G,n,e} = Mean_{zmin} & if \ S_{n,e} > 0.30 \cup R_{n,e} > 0.30 \ m \\ Z_{G,n,e} = Min_{zmin} & otherwise \end{cases} \qquad (4)$$

In the proximity of the creeks, $Mean_{zmin}$ was preferred to Min_{zmin}, avoiding the underestimation of the ground level obtained using the mean of the minimum values detected in the 3x3 stencil. In the marsh platform, where the effect of the ground elevation gradients is negligible, Min_{zmin} was preferred to $Mean_{zmin.}$

6. **STEP 6**: A correction on ground level was done as follows:

$$Z_{G,n,e} = min[z_{\min,2,2}] \qquad if \ min[z_{\min,2,2}] < z_{min,min} \qquad (5)$$

The method allows considering as valid the minimum value detected in the central cell when its elevation is lower than the values obtained using the two regression planes.

7. **STEP 7**: Finally, to remove the effect of the creeks, the $h_{i,j}$ points contained in the cells of the 1.20×1.20 m² stencil were shifted using the following procedure, obtaining a modified local point cloud:

$$\begin{cases} h_{i,j} = h_{i,j} + Z_{G,n,e} - z_{\min,i,j} & if \ z_{\min,i,j} < Z_{G,n,e} \\ h_{i,j} = h_{i,j} & if \ z_{\min,i,j} > Z_{G,n,e} \end{cases} \qquad (6)$$

The ground level and a modified point cloud in which we removed the effects of high ground-level gradients were obtained, applying the procedure to the salt marsh area. The process was done using a MATLAB based algorithm. Vegetation height was calculated as the difference between the maximum elevation value of the point cloud, and the calculated ground level in the 3x3 cell stencil. The reduction of the error in the estimation of the ground level decreases the error in the calculation of the vegetation height (Figure 2).
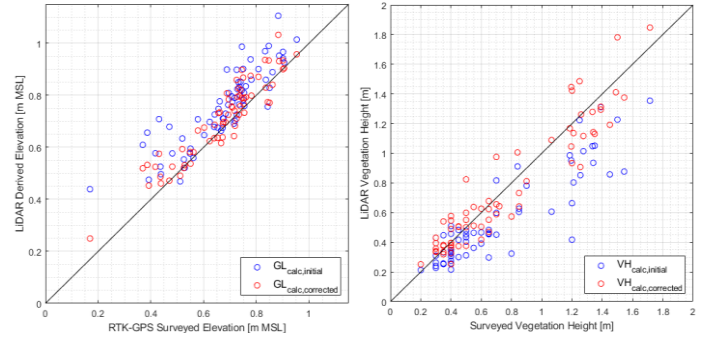
Figure 2. Displacement of ground level elevation (left) and vegetation height (right) Blue and red dots indicate the values obtained before and after the LiDAR correction.

III. RESULTS AND CONCLUSIONS

An accurate description of ground-level elevation and vegetation properties over estuarine wetlands is a crucial and challenging need in the safeguard and restoration of these delicate and useful ecosystems. Here we introduce a new algorithm for an accurate and high-resolution description of salt marshes.

The results showed in Figure 3 demonstrate as our model describes the complex tidal network of the salt marsh, producing high resolution (40×40 cm²) maps of ground elevation (Figure 3, top-right) and vegetation height (Figure 3, bottom-right), thus capturing the large gradients in the proximity of tidal creeks. As illustrated in Figure 2, the application of our corrective process considerably reduces the error in the ground level estimation. The Mean Absolute Error (MAE) decreased from 8.78 cm to 5.34 cm; the Mean Error passed from -8.2 cm to -3.9 cm; the Maximum Error lowered from 27.7 cm to 15.2 cm. As shown in Figure 2, the correction procedure results essential also to reduce the error in vegetation determination. The Mean Error lowered from 15.3 cm to 1.2 cm, the MAE changed from 18.0 cm to 11.2 cm, and the Maximum Error reduced from 78.3 cm to 34.8 cm. The considerable reduction in the determination errors proved the affordability of the developed algorithm. The performed regression analysis shows the strong relationship between the surveyed vegetation height and the value obtained from the LiDAR point cloud, with an $R^2=0.88$ and a MAE=1.7 cm. The same agreement was observed between the surveyed ground-level elevation and the value obtained from the LiDAR point cloud, with an $R^2=0.87$ and a MAE=4.4 cm. The accuracy of the acquired UAV-based LiDAR was verified using the GCPs acquired in the salt marsh using the GPS-RTK system, obtaining a maximum absolute error

of +4.4 cm and a mean absolute error of +2.0 cm, which is in agreement with the ±2 cm of vertical accuracy of the GPS station.

We want to underline as this method does not require additional datasets to perform the identification of the parameters of interest. We would also emphasize that although we have used MATLAB in the all the manipulations related to the LiDAR point cloud, our algorithm is readily reproducible in every similar source code, and does not require any special devices or commercial software. The parameters obtained by the model will then be used as a base for a more efficient description of wetlands modifications using numerical modeling strategies.
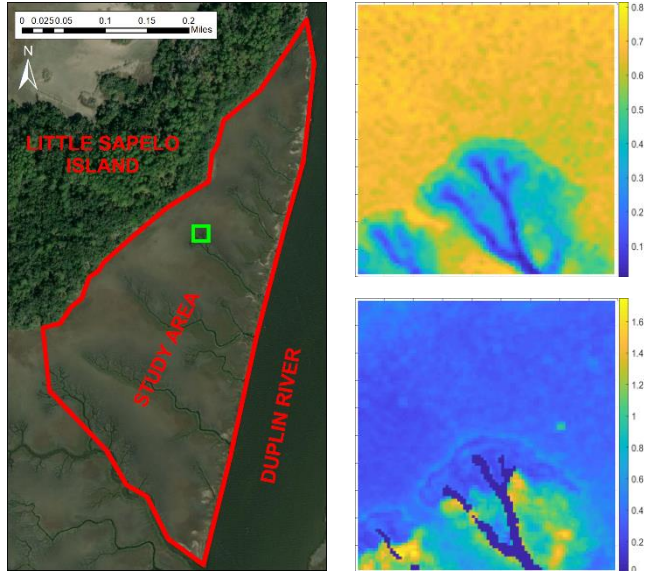
Figure 3. Example of spatial distribution of ground-level (top right) elevation and vegetation height (bottom right) calculated in a 40x40 m^2 area (green square, figure left) contained in the considered salt marsh domain (red polygon, figure left). Both parameters are displayed in meters.

REFERENCES

[1]   C. Hladik, J. Schalles, and M. Alber, "Salt marsh elevation and habitat mapping using hyperspectral and LIDAR data," *Remote Sens. Environ.*, vol. 139, pp. 318–330, 2013.

[2]   D. F. Boesch and R. E. Turner, "Dependence of fishery species on salt marshes: The role of food and refuge," *Estuaries*, vol. 7, no. 4, pp. 460–468, 1984.

[3]   L. Pendleton *et al.*, "Estimating Global 'Blue Carbon' Emissions from Conversion and Degradation of Vegetated Coastal Ecosystems," *PLoS One*, vol. 7, no. 9, 2012.

[4]   Barbier E. B., Hacker SD, Kennedy C, Koch EW, Stier AC, and Silliman BR, "The value of estuarine and coastal ecosystem services," *Ecol. Monogr.*, vol. 81, no. 2, pp. 169–193, 2011.

[5]   M. Marani, A. D'Alpaos, S. Lanzoni, L. Carniello, and A. Rinaldo, "Biologically-controlled multiple equilibria of tidal landforms and the fate of the Venice lagoon," *Geophys. Res. Lett.*, vol. 34, no. 11, pp. 1–5, 2007.

[6]   E. Mcleod, B. Poulter, J. Hinkel, E. Reyes, and R. Salm, "Sea-

[7]   S. Temmerman, G. Govers, S. Wartel, and P. Meire, "Spatial and temporal factors controlling short-term sedimentation in a salt and freshwater tidal marsh, Scheldt estuary, Belgium, SW Netherlands," *Earth Surf. Process. Landforms*, vol. 28, no. 7, pp. 739–755, 2003.

[8]   S. Temmerman, T. J. Bouma, G. Govers, Z. B. Wang, M. B. De Vries, and P. M. J. Herman, "Impact of vegetation on flow routing and sedimentation patterns: Three-dimensional modeling for a tidal marsh," *J. Geophys. Res. Earth Surf.*, vol. 110, no. 4, pp. 1–18, 2005.

[9]   S. Fagherazzi, 2 , 1 Matthew L. Kirwan, 2, 3 Simon M. Mudd, 4 Glenn R. Guntenspergen, 8 Stijn Temmerman, 5 Andrea D'Alpaos, 6 Johan van de Koppel, 7 John M. Rybczyk, and 10 and Jonathan Clough11 Enrique Reyes, 9 Chris Craft, "Numerical model of salt marsh evolution: ecological, geomorphic, and climatic factors," *Med. sans Front.*, vol. 50, no. 2011, p. 79, 2012.

[10]   M. C. Richardson, C. P. J. Mitchell, B. A. Branfireun, and R. K. Kolka, "Analysis of airborne LiDAR surveys to quantify the characteristic morphologies of northern forested wetlands," *J. Geophys. Res. Biogeosciences*, vol. 115, no. 3, pp. 1–16, 2010.

[11]   J. E. Moeslund, L. Arge, P. K. Bøcher, B. Nygaard, and J. C. Svenning, "Geographically comprehensive assessment of salt-meadow vegetation-elevation relations using LiDAR," *Wetlands*, vol. 31, no. 3, pp. 471–482, 2011.

[12]   J. E. Chassereau, J. M. Bell, and R. Torres, "A comparison of GPS and lidar salt marsh DEMs," *Earth Surf. Process. Landforms*, vol. 36, no. 13, pp. 1770–1775, 2011.

[13]   Y. Lin, J. Hyyppä, and A. Jaakkola, "Mini-UAV-borne LIDAR for fine-scale mapping," *IEEE Geosci. Remote Sens. Lett.*, vol. 8, no. 3, pp. 426–430, 2011.

[14]   G. Grenzdörffer *et al.*, "UAVs in Agriculture : Perceptions , Prospects , and " Probably Not "," *Int. Arch. Photogramm. Remote Sens. Spat. Inf. Sci.*, vol. 1, pp. 1207–1213, 2008.

[15]   M. Uysal *et al.*, "3D Shoreline Mapping Using an Unmanned Aerial Vehicle where," *FIG Congr. 2018*, vol. Conference, 2018.

[16]   J. Wang, Z. Liu, H. Yu, and F. Li, "Mapping Spartina alterniflora biomass using LiDAR and hyperspectral data," *Remote Sens.*, vol. 9, no. 6, pp. 1–14, 2017.

[17]   R. Wang and J. A. Gamon, "Remote sensing of terrestrial plant biodiversity," *Remote Sens. Environ.*, vol. 231, no. May, 2019.

[18]   D. Wang, X. Xin, Q. Shao, M. Brolly, Z. Zhu, and J. Chen, "Modeling aboveground biomass in Hulunber grassland ecosystem by using unmanned aerial vehicle discrete lidar," *Sensors (Switzerland)*, vol. 17, no. 1, pp. 1–19, 2017.

[19]   J. F. Schalles, C. M. Hladik, A. A. Lynes, and S. C. Pennings, "Landscape estimates of habitat types, plant biomass, and invertebrate densities in a Georgia salt marsh," *Oceanography*, vol. 26, no. 3, pp. 88–97, 2013.

level rise impact models and environmental conservation: A review of models and their applications," *Ocean Coast. Manag.*, vol. 53, no. 9, pp. 507–517, 2010.